Computational Design and Experimental Testing of Biological Logic Gates with Synthetic Ribozymes

An Undergraduate Thesis in the Department of Biology

Presented by Lance Lafontaine

As a Requirement for the Completion of

B. Sc. Honours in Cell and Molecular Biology

Concordia University, Montreal, Quebec, Canada

April 2014

Table of Contents

1. Abstract

Computation and the generation of logic gates in biological systems has become a focus of research in the twenty-first century due to its significant potential in synthetic biology and bioengineering. The rational bioinformatic design process for the implementation of NOR, OR, XNOR and XOR logic gates using a novel pair of ribozyme-based RNAs is proposed and assessed. The use of RNA in the generation of logic gates is advocated as a modular, expedient and flexible alternative to traditional protein or DNA enzymes. The experimental testing of the XNOR gate is realized *in vivo* and proposed *in vitro* with the targeting of the RFP mRNA as the gate output. The generation of ribozyme expression vectors is accomplished through restriction enzyme digestion and ligation experiments, and a spectrophotometric assay for the RNA regulation via transcript degradation of RFP in DH5α culture is carried out. The obtained results for the success of the XNOR gate are inconclusive and require further study regarding the efficiency of ribozyme cleavage and sequestering and spectrofluorometric assays of the RFP output signal.

2. Introduction

The recent "bottom-up" philosophy of synthetic biology has lead to a paradigm shift in how biological research is now conducted. With the simple introduction of modular genetic parts in biological systems, reliable bioengineering for a variety of functions has now become trivial and affordable. This concept of synthetic biology can thus be likened to the rise of electronic computing in the nineteenth century; modular parts with dedicated functions that can compute and solve complex systems of problems. As such, biomolecular computing and bionanotechnology have become an important topic of research in the twenty-first century.

The International Genetically-Engineered Machine (iGEM) competition is a worldwide competition encouraging students to undergo research in synthetic biology with a focus on bioengineering, innovation, education and collaboration. Concordia University competed in iGEM 2013, and I was a part of this team that helped conceive of a biological cellular automaton. *Escherichia coli* cells were designed to be universally computational by exploiting the use of amino homoserine lactones (AHLs) as biochemical inputs and outputs to a logic module. This thesis project stems from the conception of the logic module, which implemented an XOR logic gate as a means to achieve the desired output.

Logic gates are used extensively in electrical and computer engineering as a means of implementing Boolean functions in circuitry, with the purpose of accepting a varying number of inputs, performing a specific logical operation on these inputs, and predictably producing a desired output. These logic gates form the basic units of computers, as they allow for the physical representation of all Boolean logic, and render universal computation possible.

Examples of logic gates used extensively in electronics are the two-input AND, OR and XOR gates. An AND gate produces an output only when *both* inputs are present. An OR gate produces an output when *either* of two inputs are present. In comparison, an XOR gate produces an output when one and *only one* of the inputs are present. These Boolean functions can be represented in tabular format, as is seen in Table 1.

Table 1. Truth Table Representation of Boolean Logic Gates AND, OR and XOR.

AND			OR			XOR		
INPUT A	INPUT B	OUTPUT C	INPUT A	INPUT B	OUTPUT C	INPUT A	INPUT B	OUTPUT C
0	0	0	0	0	0	0	0	0
0	1	0	0	1	1	0	1	1
1	0	0	1	0	1	1	0	1
1	1	1	1	1	1	1	1	0

It is also important to note that NOT gates exist and essentially act to invert the output signal from ON to OFF and vice-versa. Surprisingly, biological NOT gates are found very commonly in genetic system, and are implemented through the use of a negative transcriptional regulator acting upon an output of interest. As such, the implementation of NAND, NOR and XNOR gates is very common and is easily achievable. The tabular representations of these logic gates are as seen in Table 2.

Table 2. Truth Table Representation of Boolean Logic Gates NAND, NOR and XNOR.

NAND			NOR			XNOR		
INPUT A	INPUT B	OUTPUT C	INPUT A	INPUT B	OUTPUT C	INPUT A	INPUT B	OUTPUT C
0	0	1	0	0	1	0	0	1
0	1	1	0	1	0	0	1	0
1	0	1	1	0	0	1	0	0
1	1	0	1	1	0	1	1	1

The successful implementation of logic gates that act expediently and reliably in biomolecular systems is an important milestone to achieve if complex computing is to be made possible in living cells. AND, OR and XOR logic gates and their NOT derivatives have been generated in many instances with the use of protein enzymes and transcription factors (Deodarine *et al*, 2003; Baron *et al*, 2006; Bronson *et al*, 2008; Stracket *et al*, 2008), DNAzymes (Bi *et al*, 2010; Elbaz *et al*, 2010; Willner *et al*, 2008; Zhu *et al,* 2011), and

DNA strand hybridization or synthesis (Okamoto *et al*, 2004; Seelig *et al*, 2006; Qian *et al*, 2001). Projects like these have often found limited applicability outside of proof of principle for one of many reasons, notably due to their lack of modularity, interaction with native cellular elements, or expedient processing of inputs and generation of an output.

It is being proposed that the use of hammerhead ribozymes is merited for the construction of biological logic gates. Ribozymes are small RNAs that catalyze chemical reactions, markedly the cleavage of other RNAs, due to their secondary structure and coordination with divalent magnesium ions (Hampel *et al*, 1997). Ribozymes have a notable viral origin, but have found in the genomes of various organisms, indicating several instances of independent evolution throughout evolutionary time (Salehi-Ashtiani *et al*, 2001).

Natural hammerhead ribozymes consist of a conserved central catalytic core, often referred to as the stem loop II. The helical stem loops I and III are naturally double-stranded and aid in the cis-cleavage of RNA. However, synthetic ribozymes can be made by reengineering stem loops I and II for the binding of a target RNA, allowing for the cleavage via the conserved stem loop II (Amarzguioui *et al*, 1998; Saksmerprome et al, 2004; Carbonell et al, 2011) of virtually any RNA sequence containing an NUH nucleotide triplet, where N can be any nucleotide and H is any nucleotide but guanine.

Natural ribozymes have very high cleavage efficiencies *in vivo.* Synthetic ribozymes, with an ideal cut site of GUC (Müller-Kuller et al, 2009), have been shown to be extremely efficient *in vitro*, and have recently seen an increase in cleavage activity *in vivo* in numerous cases (Ferbeyre *et al*, 1996; Carbonell et al, 2011; Olson *et al*, 2012; Kalweit *et al,* 2013), despite complex cellular interactions and a low concentration of magnesium cofactors (Carbonell et al, 2011).

The purpose of this study is two-fold; firstly, to provide a rational approach to the *in silico* engineering of synthetic ribozymes that operate as OR, NOR and notably XOR and XNOR gates in biological systems, and secondly, to design and implement an experimental method for the testing of the XNOR logic gate as a biological Boolean function *in vivo* and *in vitro.*

This goal began with the identification of red fluorescent protein (RFP) as a suitable logic gate output that can easily be assayed spectrophotometrically and spectrofluorometrically for in both *in vivo* and *in vitro* systems. A pair of synthetic ribozymes were also decided upon as being the two inputs to the biological logic gate.

Analogously to what is seen in an computer NOR logic gate, a biological implementation of an NOR gate can be achieved with the expression of two distinct ribozyme inputs, both targeting two separate target sites on the same RFP mRNA transcript output. As it has already been established, the presence of a ribozyme with its target RNA results

in the cleavage in the target RNA, which in this case would result in the inability of the RFP mRNA to be properly translated, which would significantly decrease the level of RFP expressed within a cell. In the described situation, the presence of either or both ribozymes would result in the decrease of RFP output, given that the ribozymes are expressed in significantly higher amounts than the RFP is, resulting in the successful realization of a biological NOR gate, as can be contrasted in Table 3.

Table 3. Comparison of Implementation of Ribozyme-Based NOR Logic Gate to Computational NOR.

COMPUTATIONAL NOR			BIOLOGICAL NOR		
INPUT A	**INPUT B**	**OUTPUT C**	**RIBOZYME A**	**RIBOZYME B**	**RFP mRNA C**
0	0	1	Absence	Absence	Intact
0	1	0	Absence	Presence	Cleaved
1	0	0	Presence	Absence	Cleaved
1	1	0	Presence	Presence	Cleaved

This implementation of a ribozyme-based biological NOR logic gate is perfectly sound, and should be able to be implemented on virtually any RNA sequence. In fact, recent experiments have ruled out the possibility of the negative effect of two RNA segments binding to one target, as this principle of combinatorial targeting of RNA is often exploited in RNAi to increase gene silencing (Win *et al*, 2009). Given the modularity of the ribozyme RNA target and the experimental reality of a biological NOR gate, the

implementation of a biological OR gate can also be easily realized by replacing the target of the ribozyme inputs to the mRNA of a transcriptional repressor such as the Lac repressor, which could negatively regulate the expression of RFP as an output.

The biological implementation of a XNOR gate (and by extension, a XOR gate) was accomplished in a very similar manner, but the challenge arose of eliminating any ribozyme activity when both ribozymes were being expressed. This difficulty was overcome with the design of what now-forth will be called "occluders" or "occluding arms". These occluders are supplementary sequences of RNA extended from the ribozyme flanking arms that allow for the strong binding of one ribozyme to the other when expressed simultaneously, therefore preventing (occluding) one another from binding to and cleaving the target RFP mRNA, allowing the latter to be successfully translated. The addition of occluders as a design feature is a novel and previously untested approach to the creation of an expedient RNA-based biological XNOR gate, as is contrasted to a computational XNOR gate in Table 4.

In addition to the conception and computation design of these biological logic gates, the *in vivo* experimental testing of the XNOR gate was designed and performed, while the *in vitro* work was solely designed due to time constraints. The *in vivo* experiments consisted of the construction of three vectors through restriction digestion and ligation, allowing for the three ribozyme input states to be generated once transformed within a

Table 4. Comparison of Implementation of Ribozyme-Based XNOR Logic Gate to Computational XNOR.

COMPUTATIONAL XNOR			BIOLOGICAL XNOR		
INPUT A	**INPUT B**	**OUTPUT C**	**RIBOZYME A**	**RIBOZYME B**	**RFP mRNA C**
0	0	1	Absence	Absence	Intact
0	1	0	Absence	Presence	Cleaved
1	0	0	Presence	Absence	Cleaved
1	1	1	Presence	Presence	Intact

competent *Escherichia coli* strain. The subsequent transformation of a separate vector into the same cultures allows for the constitutive expression of RFP within the cell. The concentration of RFP in culture was then spectrophotometrically assayed for at the absorbance wavelengths of 504nm for RFP normalized against 600nm for cell density.

The *in vitro* experiments consist of the generation of the ribozymal RNA and RFP mRNA through T7 polymerase, and examination of the resulting RNA pattern for the efficiency of ribozyme cleavage via agarose gel electrophoresis and Northern blotting if necessary.

3. Materials and Methods

3.1 *In Silico* Design

Retrieval of the DNA Sequence of Red Fluorescent Protein

The DNA sequence for an engineered monomeric mutant of RFP optimized for bacterial expression (Part Number: BBa_E1010) was obtained from the iGEM Registry of Standard Biological Parts, freely accessible at http://parts.igem.org. The part in question has 285 uses as of April 2014, and has been experimentally demonstrated to be reliable.

Analysis of Secondary Structure of RNA Transcripts

The coding sequence of RFP, as well as the synthetic ribozyme arms were uploaded for use in an online bioinformatic entitled Mfold (Zucker, 2013) freely available at http://mfold.rna.albany.edu/?q=mfold/RNA-Folding-Form. This tool allows for visualization of the two-dimensional secondary structure of an RNA sequence.

Creation of Ribozyme- and Target-Binding Ribozyme Arms

The generation of the stem loops I and III of the ribozymes that bind the RFP mRNA target, as well as the extended synthetic arms used for cross-ribozyme binding and occlusion, was accomplished through the use of the online bioinformatic tool Oligo Analyzer, a program created by IDT as a part of their SciTools suite (Owczarzy *et al*, 2008) accessible at http://www.idtdna.com/analyzer/Applications/OligoAnalyzer/. This free

software allows for the calculation of values such as sequence GC content and melting temperature, and verification of sequence hairpins, and self- and heterodimerization.

IntaRNA is another online bioinformatic tool, hosted at the University of Freiburg's Department of Computer Science website available at http://rna.informatik.uni-freiburg.de:8080/IntaRNA/Input.jsp, that performs the analysis and hybridization of two small RNA segments (Busch *et al*, 2008; Richter *et al*, 2010). This software was used for the additional verification of the correct hybridization of the ribozyme flanking arms with the RFP mRNA target.

Alignment of Ribozyme Binding Sites Against *Escherichia Coli* Genome

To ensure the specificity of the ribozyme cleavage to only RFP, the Basic Local Alignment Search Tool (BLAST) (Madden, 2003) with default parameters was used to ensure that a similar binding target and cut site did not occur in all RefSeq *E. coli*-expressed mRNA.

Verification of Restriction Enzyme Cut Sites within Ribozyme Constructs

The online tool NEBCutter by New Englands Biolabs, freely accessible at http://tools.neb.com/NEBcutter2/ (Vincze *et al*, 2003), was used in order verify the presence of various restriction endonuclease cut sites within the ribozyme constructs, in order to determine which sites should be ideal for use in later restriction digestion and ligation of the ribozyme expression cassettes.

3.2 *In Vivo* Experimental Procedures

Synthesis of the *In Vivo* and *In Vitro* Ribozyme Constructs

The DNA synthesis of the ribozyme expression constructs necessary for the following experimental procedures was performed by Life Technologies, which can be accessed at http://www.lifetechnologies.com/ca/en/home.html

The *in vivo* construct consists of two distinct ribozyme expression cassettes that are surrounded by the restriction enzyme cut sites SpeI, BamHI and EcoR1, from right to left as pictured in Figure 1. The expression cassette for Ribozyme 1 consisted of the Tet promoter (Part Number: BBa_R0040) and a transcriptional terminator (Part Number: BBa_B1006), while the Ribozyme 2 cassette consisted of the Lac promoter (Part Number: BBa_R0010) and a transcriptional terminator (Part Number: BBa_B1002). This was ordered with Life Technologies through their GeneArt® Gene Synthesis.

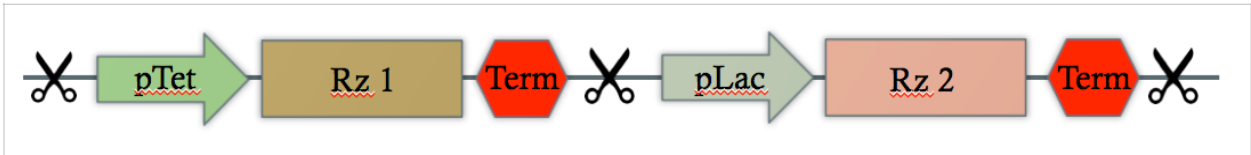

Figure 1. Representation of Synthesized Ribozyme Expression Cassettes Separated by SpeI, BamHI and EcoR1 Restriction Enzyme Cut Sites.

The *in vitro* constructs ordered through Life Technologies consisted of a series of ssDNA primers of the T7 polymerase promoter (sequence from Part Number: BBa_I719005)

followed by the ribozyme sequences, as well as primers for the amplification of the RFP coding sequence with the addition of a T7 promoter (sequence from Part Number: BBa_I719005) and Ribosome Binding Site (sequence from Part Number: BBa_B0034) upstream, and a T7 Terminator sequence (sequence from Part Number: BBa_K731721) downstream of the gene coding sequence.

Plasmid Curing of DH5αZ1 *E. coli* Culture

An undocumented DH5αZ1 strain (F-, endA1 hsdR17(rK-mK+) supE44 thi-1 λ- recA1 gyrA96 relA1 deoR, Δ(lacZYA-argF)U169, φ80dlacZΔM15, lacIq, tetR+) (Kawe et al, 2009) was obtained from a previous graduate student's work, and was unexpectedly able to grow on LB semi-solid media containing ampicillin. It was suspected that this strain was resistant to ampicillin due to a previously-transformed vector containing the ampicillin resistance gene. As a technique for the curing of this suspected plasmid, the culture was grown out and incubated at 42°C in 5mL LB and was subjected to seven sequential 1:50 serial dilutions in LB (Trevors, 1986) before successfully exhibiting non-growth on LB + ampicillin plates. A miniprep of the culture was performed at this point, the results of which indicated the lack of plasmids altogether (data not shown).

Establishing the Chemical Competency of DH5αZ1 *E. coli* Cells

The obtained cured DH5αZ1 culture was then made chemically competent for transformation with a calcium chloride procedure. 1mL of culture was centrifuge for 5 minutes at 4,000 rpm at room temperature. The cell pellet was resuspended in 1mL of cold

$CaCl_2$. The cells were once again centrifuged and resuspended in cold $CaCl_2$ in the same manner (Variation on Concordia University Department of Biology, 2014).

Restriction Endonuclease Digestion of Ribozyme Construct and Vector

Three distinct instances of restriction enzyme digestion of the synthesized ribozyme cassettes and the pBluescript KS II (+) vector were carried out, with all possible double combinations of the NEB restriction endonucleases SpeI, BamHI and EcoRI. This would result in the generation of three separate constructs containing one single ribozyme expression cassette, the other single ribozyme expression cassette, and one construct containing both ribozyme expression cassettes, as well as the generation of the appropriately-cut pBluescript vector for subsequent insert cloning. Each restriction digestion reaction totalled to 20uL, with 2uL of 10X NEB Buffer 2, 1uL UltraPure H_2O, 1uL of each appropriate restriction enzyme, and 15uL undigested DNA, and was incubated at room temperature for one to two hours (Variation on Concordia University Department of Biology, 2014).

Ligation Reaction of Ribozyme Constructs and Vector

The ligation reactions for the three instances of cloning of the ribozyme construct inserts into the cut pBluescript vectors were performed with an ideal ligation reaction vector:insert ratio of 1:3 in consideration. The reaction totalled to 20uL, with 2uL 10X NEB T4 ligase buffer, 13uL UltraPure H_2O, 1uL T4 ligase, 2.7uL digested insert DNA and 1.3uL

digested vector DNA, which was incubated at room temperature overnight (Variation on Concordia University Department of Biology, 2014).

Transformation of Competent DH5αZ1 and DH5α Cultures

The transformation of the ligation reactions occurred by initially pipetting 5uL of each ligation reaction into 100uL of DH5αZ1, and subsequently DH5α cultures. The cells were iced for 30 minutes and then subjected to a 42°C water bath for 2 minutes. After being placed on ice again, 900mL of LB was added to each transformation reaction, which were incubated at 37°C for 45 minutes. 150uL of each transformed culture was plated onto LB semi-solid media containing ampicillin and a top layer of 40uL 1M IPTG and 40uL X-Gal at 20ug/uL in DMSO, and incubated for 24 hours at 37°C. (Variation on Concordia University Department of Biology, 2014).

Miniprep of Three Desired Ribozyme Constructs and Analysis of Transformed Vectors

Minipreps of all three vectors with ribozyme expression cassette inserts were performed for storage and future use with a Qiagen miniprep and gel extraction kit. All procedures were followed as indicated in the kit's manual. The plasmid sample obtained from the miniprep were then analyzed by electrophoresis on a 1% agarose gel at 100V for approximately one hour and twenty minutes. The resulting gel was then photographed in a ultraviolet transilluminator.

Establishment of Chemical Competency and Double Transformation of RFP Vector into DH5α Cultures

The DH5α cultures previously transformed with the three distinct ribozyme-pBluescript vectors were made chemically competent for another transformation via the same procedure as described earlier. An RFP expression cassette in a vector, previously obtained through iGEM 2013, was then transformed into the DH5α cells and plated onto LB semi-solid media containing both chloramphenicol and ampicillin, via the same procedure as described previously. This RFP expression cassette (Part Number: BBa_K516132) contains a medium efficiency constitutive promoter (Part Number: BBa_J23101), a medium efficiency Ribosome Binding Site (Part Number: BBa_B0032), the RFP coding sequence as seen in Figure X (Part Number: BBa_E1010), and a double transcriptional terminator (Part Numbers: BBa_B0010 and BBa_B0012), as is seen in Figure 2. This particular construct was obtained through the iGEM 2013 distribution kits, and was shipped cloned into an iGEM plasmid backbone called pSB1C3.

Cell Growth Time Course and Spectrophotometric Assay for RFP

At the time of the previously described double transformations and platings, a single transformation into DH5α was also performed and subsequently plated onto semi-solid media with the appropriate selection markers with the same procedure as described previously, but with a pUC19 (ampicillin) plasmid and with the RFP-pSB1C3 (chloramphenicol) vector alone. Upon growth of the plates at 37°C for 24 hours, colonies observed from the pUC19 transformation, the RFP single transformation, and the

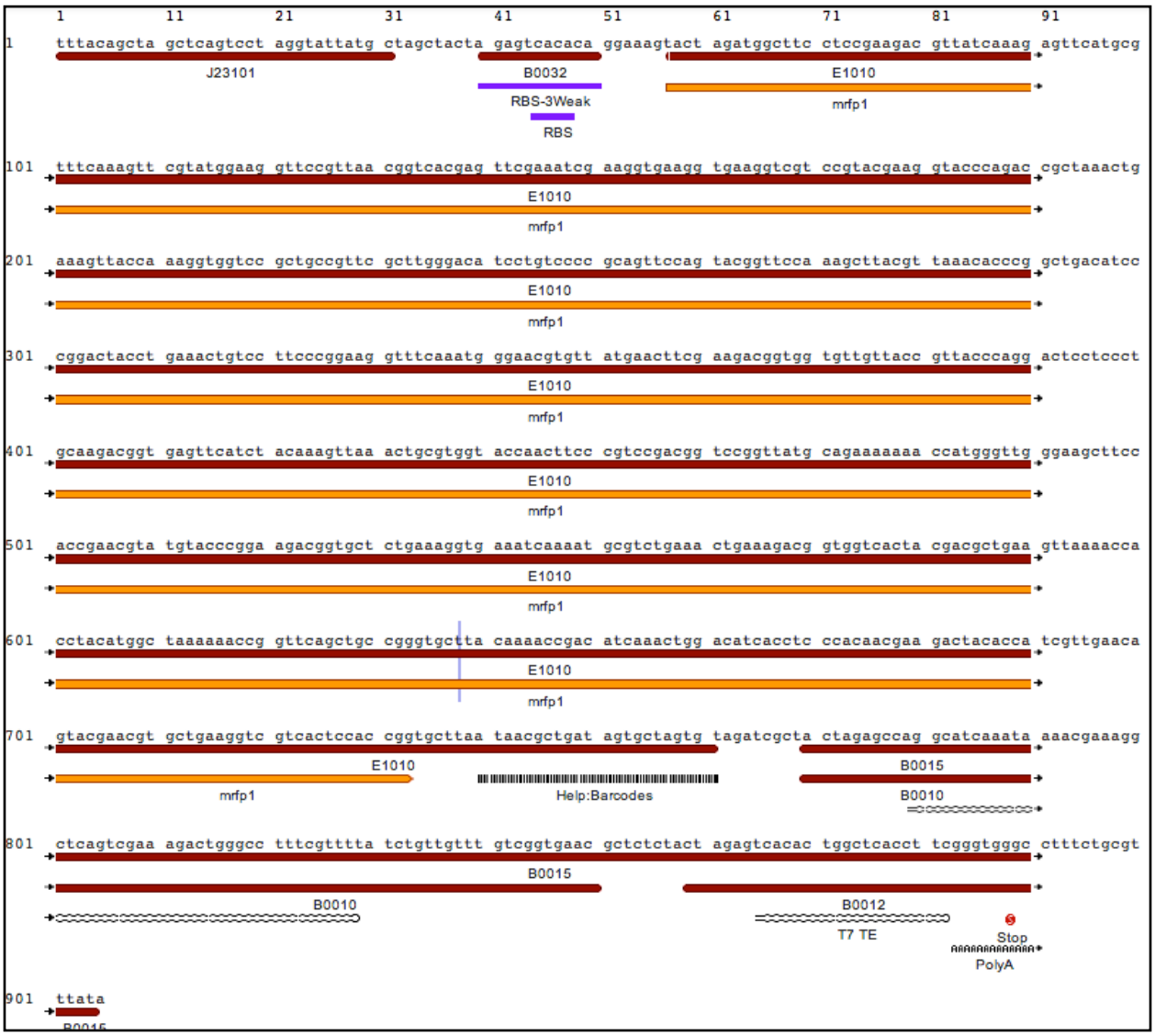

Figure 2. RFP Expression Cassette (Part Number: BBa_K516132), as seen on the Registry of Standard Biological Parts.

lac-regulated ribozyme and RFP double transformation were picked and outgrown in LB liquid media with appropriate antibiotics for 45 minutes, after which the time course commenced.

A 2013 iGEM team at the Harbin Institute of Technology in China had performed successful experiments involving the detection of RFP expressed in culture via spectrophotometry, with the goal of creating a novel transcription factor-based AND gate. Figure 3 describes the results of their experiment describing the linear relationship between the relative concentration of the same engineered RFP gene (Part Number: BBa_E1010) expressed at different concentrations and the absorbance of the cultures at 504nm, normalized for the cell density at 600nm (iGEM HIT-Harbin, 2013).

This same strategy was used in this experiment for the assay of the variation in concentration of RFP due to mRNA degradation by ribozymes. The absorbance values at 504nm and at 600nm of the three cultures in question as previously mentioned were obtained with a spectrophotometer over a course of five hours.

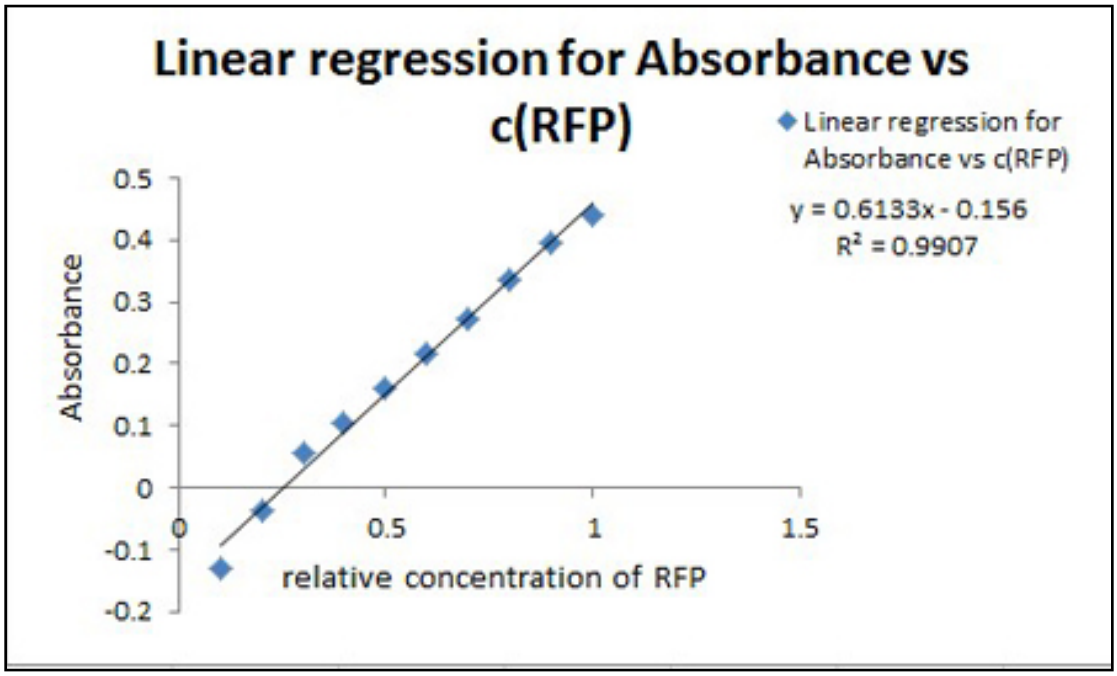

Figure 3. The Standard Curve for Detection of Expressed RFP in *E. coli* Cultures via Spectrophotometry at 504nm, Normalized for Cell Density at 600nm.

4. Results

4.1 *In Silico* Design

This study began with isolation of the coding sequence of a highly-engineered red fluorescent protein from the iGEM Registry of Standard Biological Parts, as can be seen in Figure 4. The transcribed mRNA sequence of this gene is to be the designed output of the biological logic. This sequence was targeted for cleavage by a hammerhead ribozyme catalytic core (Saksmerprome *et al*, 2004), and thus all GUC nucleotide triplets within the sequence were identified (Müller-Kuller et al, 2009), as can be seen in Figure 5.

```
ATGGCTTCCTCCGAAGACGTTATCAAAGAGTTCATGCGTTTCAAAGTTCGTATGGAAGGT
TCCGTTAACGGTCACGAGTTCGAAATCGAAGGTGAAGGTGAAGGTCGTCCGTACGAAGGT
ACCCAGACCGCTAAACTGAAAGTTACCAAAGGTGGTCCGCTGCCGTTCGCTTGGGACATC
CTGTCCCCGCAGTTCCAGTACGGTTCCAAAGCTTACGTTAAACACCCGGCTGACATCCCG
GACTACCTGAAACTGTCCTTCCCGGAAGGTTTCAAATGGGAACGTGTTATGAACTTCGAA
GACGGTGGTGTTGTTACCGTTACCCAGGACTCCTCCCTGCAAGACGGTGAGTTCATCTAC
AAAGTTAAACTGCGTGGTACCAACTTCCCGTCCGACGGTCCGGTTATGCAGAAAAAAACC
ATGGGTTGGGAAGCTTCCACCGAACGTATGTACCCGGAAGACGGTGCTCTGAAAGGTGAA
ATCAAAATGCGTCTGAAACTGAAAGACGGTGGTCACTACGACGCTGAAGTTAAAACCACC
TACATGGCTAAAAAACCGGTTCAGCTGCCGGGTGCTTACAAAACCGACATCAAACTGGAC
ATCACCTCCCACAACGAAGACTACACCATCGTTGAACAGTACGAACGTGCTGAAGGTCGT
CACTCCACCGGTGCTTAATAA
```

Figure 4. DNA Coding Sequence of Engineered Monomeric Mutant of RFP Optimized for Bacterial Expression (Part Number: BBa_E1010).

AUGGCUUCCUCCGAAGACGUUAUCAAAGAGUUCAUGCGUUUCAAAGUUCGUAUGGAAGGU
UCCGUUAACG**GUC**ACGAGUUCGAAAUCGAAGGUGAAGGUGAAG**GUCGUC**CGUACGAAGGU
ACCCAGACCGCUAAACUGAAAGUUACCAAAGGUG**GUC**CGCUGCCGUUCGCUUGGGACAUC
CU**GUC**CCCGCAGUUCCAGUACGGUUCCAAAGCUUACGUUAAACACCCGGCUGACAUCCCG
GACUACCUGAAACU**GUC**CUUCCCGGAAGGUUUCAAAUGGGAACGUGUUAUGAACUUCGAA
GACGGUGGUGUUGUUACCGUUACCCAGGACUCCUCCCUGCAAGACGGUGAGUUCAUCUAC
AAAGUUAAACUGCGUGGUACCAACUUCCC**GUC**CGACG**GUC**CGGUUAUGCAGAAAAAAACC
AUGGGUUGGGAAGCUUCCACCGAACGUAUGUACCCGGAAGACGGUGCUCUGAAAGGUGAA
AUCAAAAUGC**GUC**UGAAACUGAAAGACGGUG**GUC**ACUACGACGCUGAAGUUAAAACCACC
UACAUGGCUAAAAAACCGGUUCAGCUGCCGGGUGCUUACAAAACCGACAUCAAACUGGAC
AUCACCUCCCACAACGAAGACUACACCAUCGUUGAACAGUACGAACGUGCUGAAG**GUC**GU
CACUCCACCGGUGCU

Figure 5. Sequence of mRNA Transcript of Engineered Monomeric Mutant of RFP Optimized for Bacterial Expression (Part Number: BBa_E1010), where all GUC ribozyme cleavage sites are underlined and bolded.

This mRNA transcript was then subjected to a bioinformatic tool called Mfold (Zucker, 2013) for the determination of the most likely secondary structure of the transcript in cellular conditions. The output of this manipulation can be seen in Figure 6, where the most stable configuration of the transcript is shown, with a Gibb's free energy of -207.20 kcal/mol.

Two ideal ribozyme cut sites were established based on factors such as their accessibility in the secondary structure of the transcript, their efficient cut sites, non-repetitive adjacent sequences, and proximity to one another. The RNA sequences of these cleavage sites are shown in Figures 7 and 8.

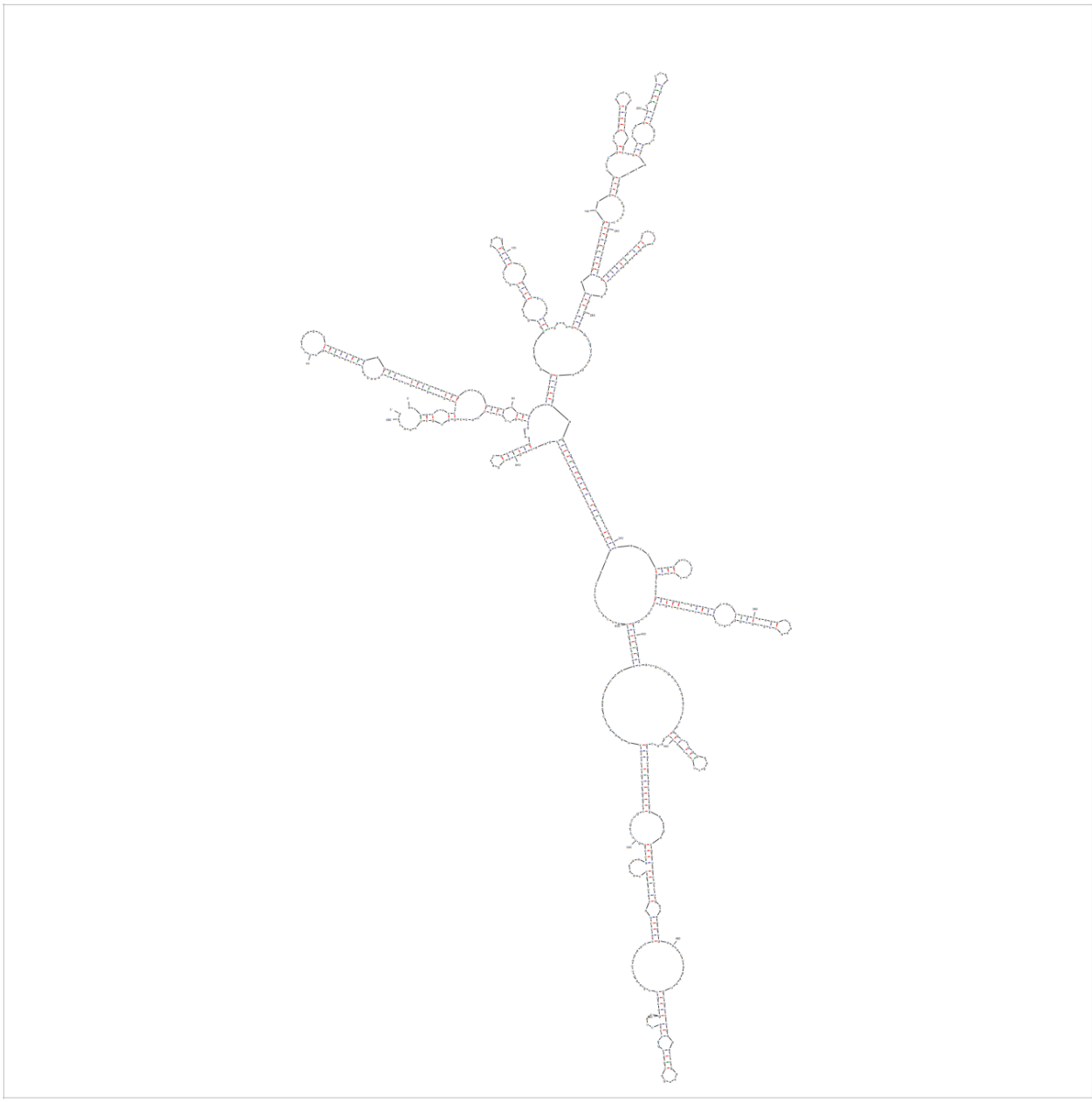

Figure 6. Most Stable Theoretical Secondary Structure of mRNA Transcript of RFP (Part Number: BBa_E1010) in Cellular Conditions.

GGUUCCGUUAACG**GUC**ACGAGUUCGAAAU

Figure 7. GUC Cut Site and Adjacent Sequences on RFP mRNA Transcript As Target for Ribozyme 1.

GAAAUCAAAAUGC**GUC**UGAAACUGAAAGA

Figure 8. GUC Cut Site and Adjacent Sequences on RFP mRNA Transcript As Target for Ribozyme 2.

The target-binding flanking arms of each ribozyme were then generated by taking the reverse complementary sequence of the sequences adjacent to the chosen cut sites, as seen in Figures 9 and 10. The melting temperature of each adjacent sequence had a variable melting temperature of binding between 38.8°C and 47.2°C, with the entirety of the flanking arms ranging between melting temperatures of 56.4°C and 64.4°C, as calculated by IDT's Oligo Analyzer, a software program available as a part of the SciTools suite (Owczarzy *et al*, 2008).

AUUUCGAACUCGU_**AC**CGUUAACGGAACC

Figure 9. Target-Binding Ribozyme 1 Flanking Arms, where "_" represents the lack of a nucleotide for the future insertion of the catalytic stem loop (Saksmerprome et al, 2004), and the bolded and underlined sequence is complementary to the target GUC.

UCUUUCAGUUUCA_**AC**GCAUUUUGAUUUCA

Figure 10. Target-Binding Ribozyme 2 Flanking Arms, where "_" represents the lack of a nucleotide for the future insertion of the catalytic stem loop (Saksmerprome et al, 2004), and the bolded and underlined sequence is complementary to the target GUC.

The following step requires the addition of stem loop II to the binding arms of the ribozyme, as it is required for the catalysis of RNA cleavage. The sequence of the catalytic ribozyme core as well as a UAA bump required for efficient cleavage was obtained (Saksmerprome et al, 2004) and inserted into the current RNA build, as seen in Figures 11 and 12. Once inserted, the ribozymes are fully functional, and should experimentally be able to cleave the target sequence upon binding.

UAUUUCGAA**UAA**CUCGU**CUGAUGAGUCGCUGAAAUGCGACGAA**ACCGUUAACGGAACC

Figure 11. Functional Form of Ribozyme 1 (Flanking Arms and Catalytic Core), where the bolded and underlined sequences form the UAA bump and the stem loop II.

UCUUUCAG**UAA**UUUCA**CUGAUGAGUCGCUGAAAUGCGACGAA**ACGCAUUUUGAUUUCA

Figure 12. Functional Form of Ribozyme 2 (Flanking Arms and Catalytic Core), where the bolded and underlined sequence form the UAA bump and the stem loop II.

As previously mentioned, having two ribozymes as inputs targeting and cleaving the same RFP mRNA as an output functions as an implementation of a NOR gate. Further studies would include the experimental testing of the two functionally-complete ribozymes as proposed in Figures 11 and 12 *in vitro* and *in vivo* for proper function as a biological NOR gate.

To ensure that the ribozymes are truly specific to only RFP mRNA, a Basic Local Alignment Search Tool (BLAST) (Madden, 2003) with default parameters was initiated on a database of all RefSeq *E.coli* mRNA. No significant hits were found for Ribozymes 1 or 2 (data not shown).

The additional computational design of occluders is specific to the implementation of the XNOR gate. As can be seen in Figures 13 and 14, the occluders on each individual ribozyme are composed of only purine bases or only pyrimidine bases. However, it displays perfect complementarity and a high binding affinity between the occluders on different ribozymes, allowing for the occlusion of the pair of ribozymes and their sequestering from the target mRNA. These occluder sequence have a strong binding affinity with a high melting temperature of approximately 60°C for each pair of occluders. These melting temperatures should theoretically favour the hybridization of a ribozyme with it's ribozyme counter as opposed to the target mRNA, given a choice. An cartoon-like computer-generated drawing representing the biological state in which both XNOR ribozymes are simultaneously expressed is shown in Figure 15.

AAAAGGAGGAAAGGGAAGGAGUAUUUCGAAUAACUCGUCUGAUGAGUCGCUGAAAUGCGA
CGAAACCGUUAACGGAACC**GAGGAAGGGAAAGGAGGAAAA**

Figure 13. Functional Form of XNOR Ribozyme 1 With Additional Occluders At Extremities, where the bolded and underlined sequences are the occluders.

UUUUCCUCCUUUCCCUUCCUCUCUUUCAGUAAUUUCACUGAUGAGUCGCUGAAAUGCGAC
GAAACGCAUUUUGAUUUCA**CUCCUUCCCUUUCCUCCUUUU**

Figure 14. Functional Form of XNOR Ribozyme 1 With Additional Occluders At Extremities, where the bolded and underlined sequences are the occluders.

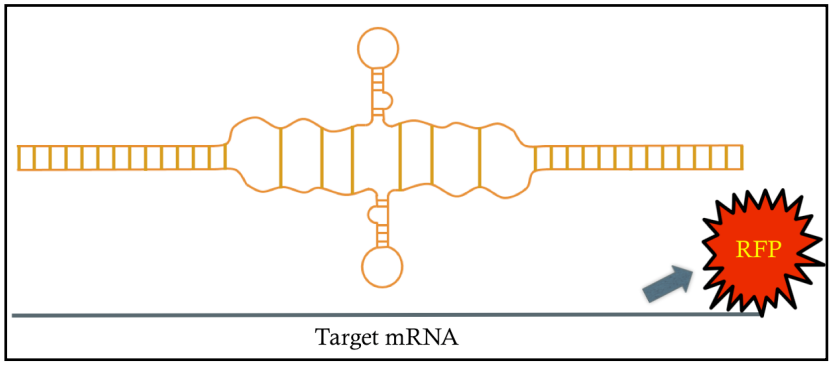

Figure 15. Cartoon Representation of Interaction of Two XNOR-Designed Ribozymes on Target RFP mRNA (**not** representative of reality).

4.2 *In vivo* Experimental Procedures

The *in vivo* experiments began with the synthesis of a ribozyme construct with Life Technologies. The construct, as can be visualized in Figure X, consists of expression for each ribozyme, under the control of the Lac (Part Number: BBa_R0010) and Tet (Part Number: BBa_R0040) promoters. The two expression cassettes were separated by the SpeI, BamH1 and EcoR1 restriction enzyme cut sites, from 5' to 3'. The entire sequence of the above construct is shown in Figure 16.

```
CCGTATACTAGTTCCCTATCAGTGATAGAGATTGACATCCCTATCAGTGATAGAGATACT
GAGCACAAAAGGAGGAAAGGGAAGGAGTATTTCGAATAACTCGTCTGATGAGTCGCTGAA
ATGCGACGAAACCGTTAACGGAACCGAGGAAGGGAAAGGAGGAAAAAAAAAAAAACCCCG
CCCCTGACAGGGCGGGGTTTTTTTTGGATCCCAATACGCAAACCGCCTCTCCCCGCGCGT
TGGCCGATTCATTAATGCAGCTGGCACGACAGGTTTCCCGACTGGAAAGCGGGCAGTGAG
CGCAACGCAATTAATGTGAGTTAGCTCACTCATTAGGCACCCCAGGCTTTACACTTTATG
CTTCCGGCTCGTATGTTGTGTGGAATTGTGAGCGGATAACAATTTCACACATTTTCCTCC
TTTCCCTTCCTCTCTTTCAGTAATTTCACTGATGAGTCGCTGAAATGCGACGAAACGCAT
TTTGATTTCACTCCTTCCCTTTCCTCCTTTTCGCAAAAAACCCCGCTTCGGCGGGGTTTT
TTCGCGAATTCGACTGA
```

Figure 16. Sequence of the Synthesized *In Vivo* Ribozyme Construct.

To ensure the successful restriction digestion of the ribozymes and cloning into their appropriately-digested vectors, this sequence was subjected to the online bioinformatic tool NEBCutter (Vincze *et al*, 2003), which allowed for the identification of all restriction enzyme cut sites within the sequence. The output of this software can be seen in Figure 17. All three expected cut sites (SpeI, BamHI, EcoR1) appear in the proper order and

at the expected locations, and no other occurrences of these sites are present, indicating the theoretical successful digestions of these ribozyme expression cassettes for cloning.

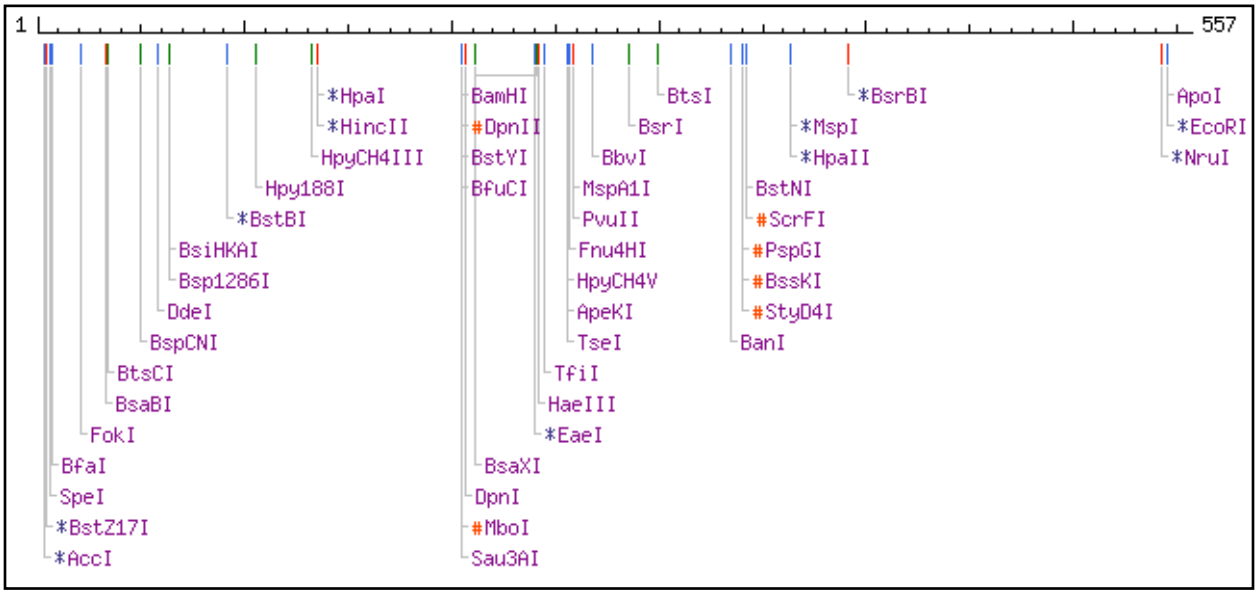

Figure 17. Identification of Restriction Enzyme Cut Sites Within Ribozyme Construct for Assurance of Proper Cloning.

The use of the DH5αZ1 *E. coli* strain was warranted due its incorporation and expression of the Tet repressor. The strain was initially obtained uncharacterized from a previous graduate student's work. The strain's mysterious ability to grow on ampicilin media was remarked, and the presence of a plasmid in the strain was suspected. A technique for plasmid curing was attempted (Trevors, 1986), involving the growth of the culture in liquid LB media without antibiotics at 42°C. Seven 1:50 sequential serial dilutions ensued at 12 to 24 hour intervals. The culture was assayed for growth on LB semi-seolid media containing ampicillin for the last few dilutions, and eventually resulted in no

growth. A plasmid miniprep of the culture ensued, in which no bands were detected (data not shown). This plasmid-cured culture was then made chemically competent with calcium chloride.

The restriction digestion of the synthesized ribozyme construct as seen in Figures 1 and 16, as well as the pBluescript KS II (+) vector to be used as a plasmid backbone, was performed. Three separate instances of the digestion (SpeI+BamHI, SpeI+EcoRI, BamHI+EcoRI) of the construct and vectors resulted in generation of each ribozyme expression cassette, and one construct containing both expression cassettes, with the appropriate cut sites for simple directional cloning into the multiple cloning site of the pBluescript vector. The vector map of pBluescript can be seen in Figure 18. The MCS of pBluescript interrupts the beta-galactosidase enzyme, allowing for the future blue/ white screening of vectors containing an insert. The vector also expresses the ampicillin resistance gene, allowing for future selection of transformed cells on LB plates.

The digested ribozyme constructs and their respective cut vectors were subjected to a ligation reaction with T4 ligase. The transformation of the samples resulting from the ligation were then performed into the prepared chemically-competent DH5αZ1 cultures, subsequently plated onto LB media containing ampicillin, IPTG and X-Gal, and were incubated at 37°C for 24 hours. Unfortunately, no colonies arose for the transformant cells of any of the three ligation reactions.

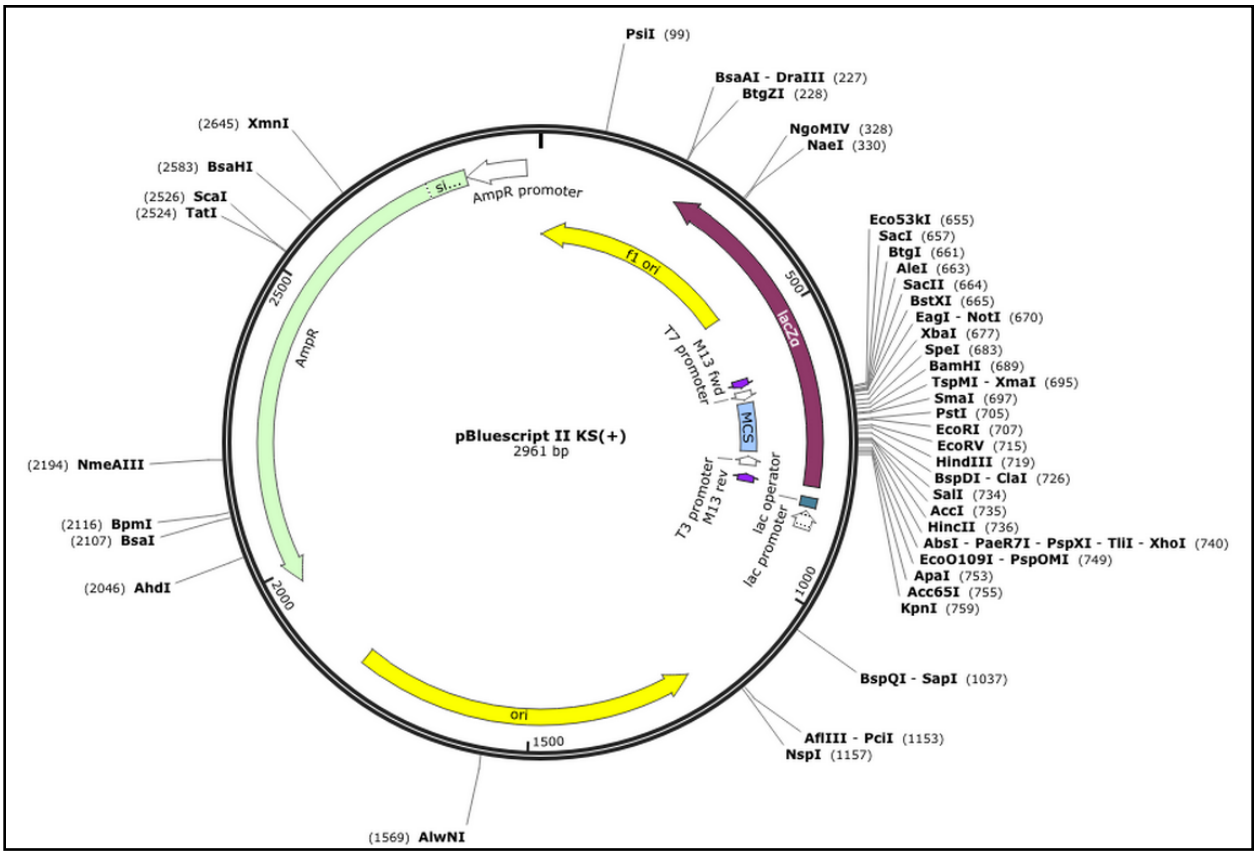

Figure 18. Vector Map of pBluescript II KS (+) with Annotated Features (SnapGene, 2014).

A new batch of plasmid-cured DH5αZ1 were made competent with the same procedure as previously performed, and were transformed and plated with the ligation reactions as previously done, but once again, no growth was observed. Due to the time constraints of the project, the transformation reactions were performed once more with the same procedure in an chemically-competent TOP10 DH5α strain obtain from previous work in iGEM 2013. The growth of the colonies are as described in Table 5, where the undigested pUC19 was used as a positive control for transformation, and water was used as a negative control.

Table 5. Transformation of DH5α *E. coli* Strain with Ribozyme and Vector Ligation Products and Appropriate Controls.

Type of Ligation Transformed	Number of Blue Colonies	Number of White Colonies
Ribozyme 1	18	30
Ribozyme 2	23	20
Ribozyme 1+2	25	19
pUC19	84	1
Water	0	0

After the successful transformation and growth of the DH5α cultures as previously described, colonies were picked from the Ribozyme 1, Ribozyme 2 and Ribozyme 1+2 transformations and subject to a plasmid miniprep for the isolation and storage for future use of the ribozyme-pBluescript vectors. The obtained plasmid were then electrophorized on a 1% agarose gel to verify the expected sizes between approximately 2900 and 3400 base pairs. The gel was then photographed using an ultraviolet transilluminator, as can be seen in Figure 19.

The DH5α cultures previously transformed with the ribozyme-pBluescript vectors were rendered chemically-competent with calcium chloride with the same procedure as used before, and an RFP expression cassette (Part Number: BBa_K516132), as seen in Figure 2, cloned into the vector pSB1C3 was transformed into all three distinct cultures.

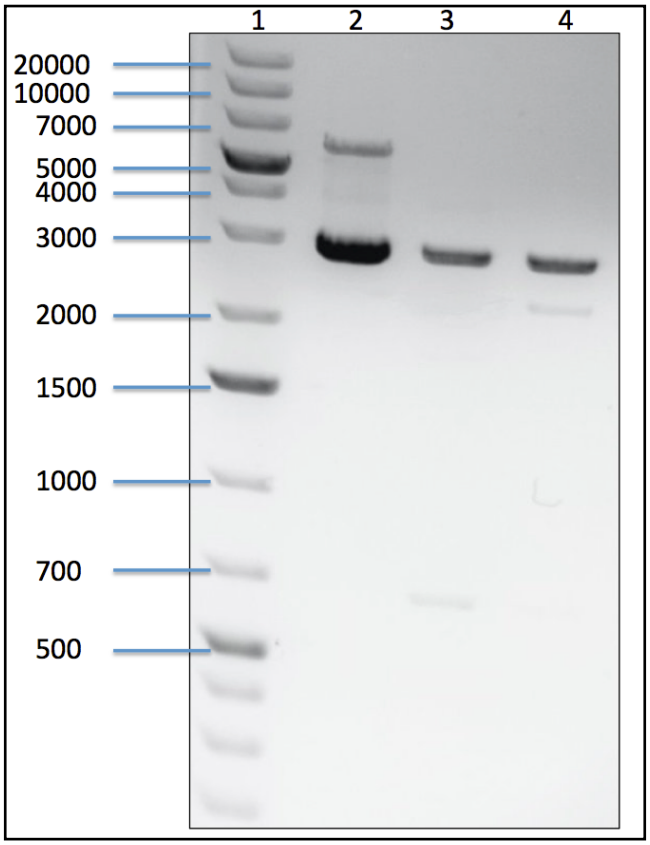

Figure 19. Agarose Gel Electrophoresis of Miniprepped Vectors from DH5α Cells Transformed with Ribozyme Constructs, where lane 1 represents a Thermo Scientific GeneRuler 1kb Plus DNA ladder (Catalog Number SM1331), lane 2 represents miniprepped sample of Ribozyme 1 vector, lane 3 represents miniprepped sample of Ribozyme 2 vector, and lane 4 represents miniprepped sample of Ribozyme 1+2 vector.

This plasmid was obtained as a part in the iGEM 2013 distribution kit, and no recombination was necessary for the purpose of this experiment. The vector map of the pSB1C3 vector with functional features annotated can be seen in Figure 20. This plasmid features a chloramphenicol resistance gene for transformant selection, and an innovative

BioBricks prefix and suffix, allowing for the control of orientation and order of sequential insert cloning. (Gasiūnaitė *et al*, 2013).

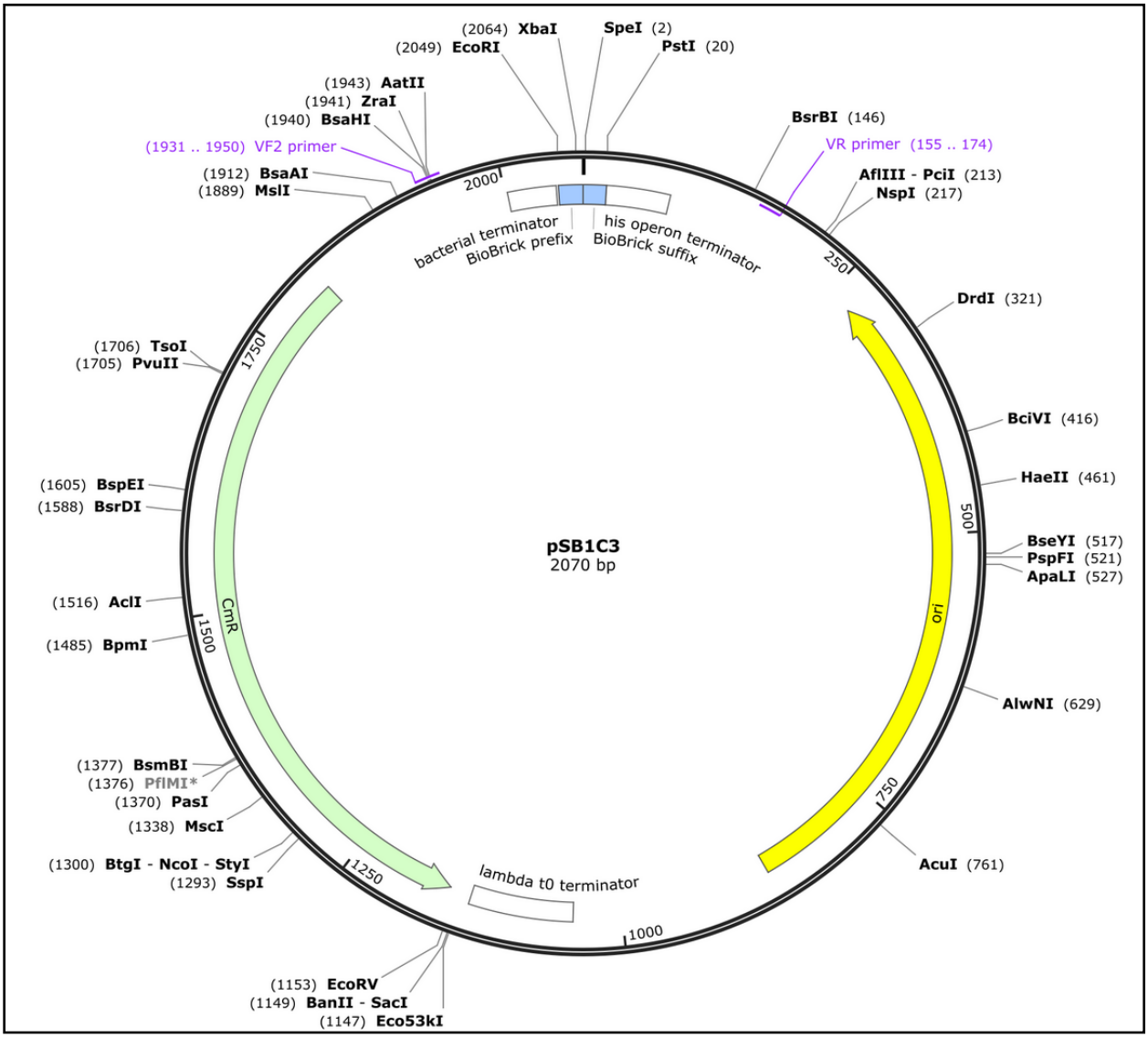

Figure 20. Plasmid map of pSB1C3 with Annotated Features (SnapGene, 2014).

Following the transformation of the RFP expression cassette (Part Number: BBa_K516132), the three separate cultures containing the three distinct ribozyme vectors and the RFP vector were plated onto LB semi-solid media complemented with

ampicillin and chloramphenicol for the selection of both plasmids, and grown at 37°C for 24 hours. Similarly, TOP10 DH5α cells were also used to transform a pUC19 vector, as well as the RFP-pSB1C3 plasmid alone, which were subsequently plated on adequate media. The resulting growth of colonies on these plates is displayed in Table 6.

Table 6. Sequential Transformation of DH5α *E. coli* Strain with RFP-pSB1C3 Vector.

Type of Vectors Transformed	**Type of Antibiotics in Media**	**Number of Colonies**
Ribozyme 1 and RFP	Chloramphenicol and Ampicillin	0
Ribozyme 2 and RFP	Chloramphenicol and Ampicillin	4
Ribozyme 1+2 and RFP	Chloramphenicol and Ampicillin	0
RFP	Chloramphenicol	9
pUC19	Ampicillin	72

A spectrophotometric assay for RFP was conducted only with the Ribozyme 2 and RFP double transformant, the RFP transformant and the pUC19 transformant, as no colonies were observed on the other plates. The experiment was not performed once more due to time constraints. The three cultures in question were picked from the plate, outgrown in

LB media with the appropriate antibiotics for 45 minutes, and were spectrophotometrically assayed at this point deeemed Time 0. This assay was based on previous studies done by the Harbin Institute of Technology iGEM 2013 team (iGEM HIT-Harbin, 2013). The assay for RFP consisted of the measurement of absorbance at wavelengths 504nm for RFP detection and 600nm for cell density detection of the three growing cultures for five hours, which are reported in Table 7 and graphically presented in Figure 21.

Table 7. Absorbance Values for Spectrophotometric Assay of RNA Regulation of RFP Signal in Culture.

	Types of Vectors Transformed								
	pUC19			RFP			RFP and Ribozyme 1		
Time (hours)	Abs 504nm	Abs 600nm	504nm / 600nm	Abs 504nm	Abs 600nm	504nm / 600nm	Abs 504nm	Abs 600nm	504nm/ 600nm
1	0.243	0.197	1.2335	0.366	0.250	1.4640	0.355	0.217	1.6359
2	0.463	0.386	1.1994	0.534	0.322	1.6584	0.584	0.366	1.5956
3	0.540	0.417	1.2950	0.688	0.408	1.6863	0.704	0.454	1.5507
4	0.636	0.475	1.3390	0.780	0.507	1.5385	0.845	0.516	1.6376
5	0.832	0.631	1.3185	0.948	0.629	1.5072	0.996	0.608	1.6382

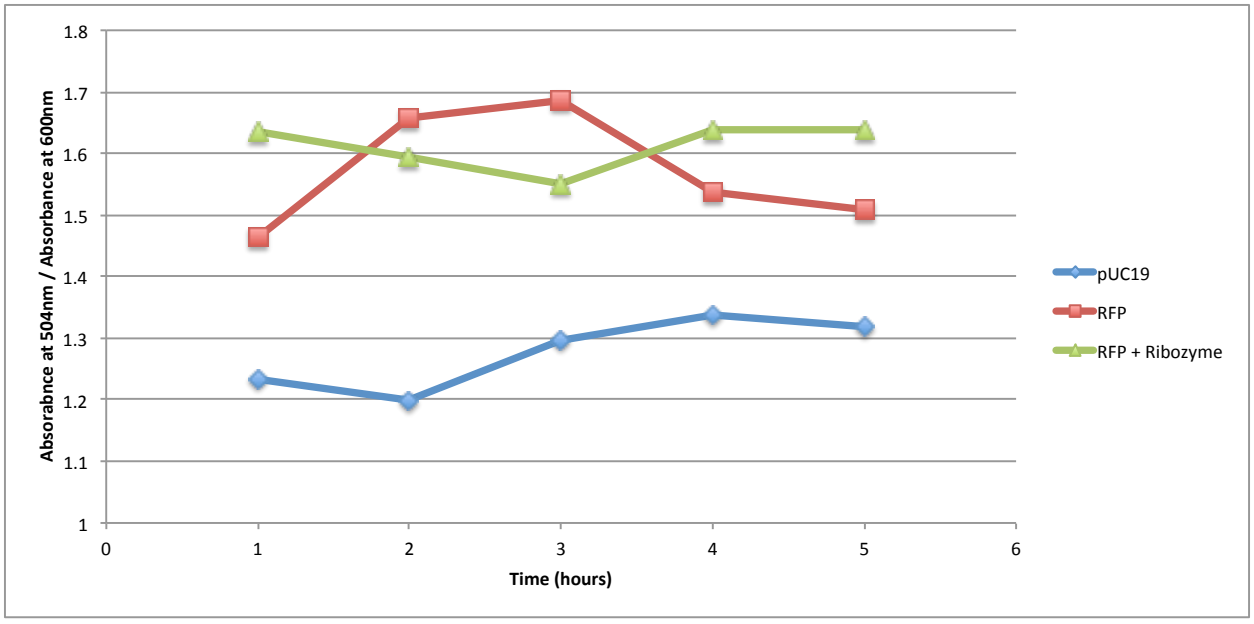

Figure 21. Spectrophotometric Assay of RNA Regulation of RFP Signal in Culture.

5. Discussion

The goal of this study was two-fold. The first objective was to conceive of the rational and systematic design of NOR, OR, XNOR and XOR logic gate in biological systems using ribozymes as a medium, and to assess the feasibility of this *in silico* model. The second goal was to experimentally verify the efficiency of the ribozyme-based XNOR gate *in vivo* while using the RFP mRNA as a target output for the logic gate.

The design of the ribozyme logic gates began with the acquisition of the RFP sequence from the iGEM Registry of Standard Biological parts, as this DNA sequence is the first step in this systematic design. From a rational point of view, one must always begin the design process with a target sequence, as trans-cleaving ribozymes must bind to a sequence to be of any use at all. The step of finding all GUC sequences must also come next, as they are the locations of highest probability of efficient ribozyme cleavage.

The folding and determination of the secondary structure of the mRNA transcript with Mfold (Zucker, 2003) is an additional step in the design process that theoretically increases the likelihood of RFP mRNA degradation. This step may not be essential for an the execution of efficient logic gate, and may be eliminated if future studies suggest that it's usefulness is moot. The fact that many other possible folding configurations of the transcript in a dynamic cellular system are possible was considered. Nonetheless, the selection of the most ideal ribozyme cut sites was performed with only one of many possi-

ble secondary structures, as it is the most thermodynamically-stable structure for this particular mRNA.

The length of the target-binding ribozyme flanking arms were specifically chosen in order to bind at a lower affinity (lower melting temperature) that the significantly longer occluder sequences which were designed to bind with a higher affinity (higher melting temperature).

As the synthetic sequence of the stem loops I and III (the target-binding ribozyme flanking arms) is highly variable and specific to your sequence of choice, the simple insertion of the conserved sequence for the catalytic loop (Saksmerprome *et* al, 2004) at the centre of both flanking arms was an unexpected attractive design feature, allowing for increased modularity in the cleavage of virtually any RNA with an NUH nucleotide triplet.

The additional of the occluders specific to the XNOR gate allows for occlusion and sequestering of the ribozymes from the target RFP mRNA due to their particularly strong binding affinity for one another. Due to the fact that both occluders on a single ribozyme are made of either only purines or pyrimidines, no binding can possibly occur between the sequence within an occluder, and between occluders on the same ribozyme. This prevents the formation of any secondary structure competing with the binding of the catalytic loop, and well as the hybridization of the target with the target, but

strongly encourages the binding of ribozymes to one another due to their perfect complementarity and high melting temperatures. In addition, the added design feature of the staggered increasing number of altered bases, as seen in Figures 13 and 14, prevent the slippage of occluder hybridization, leading to a more reliable cross-ribozyme binding.

The sequence arrangement in the synthesized ribozyme expression cassettes was constructed with the intention of easily performing three distinct restriction digest and ligation reactions to result in the three desired ribozyme expression vectors, which each represent one of the input states within an XNOR logic as seen in Table 4. This experimental method was constructed for the simple transformation of these three vectors, resulting in the direct addition of the XNOR gate inputs within a cellular system.

The pBluescript II KS (+) plasmid used in the cloning of the ribozyme cassettes was specifically chosen due to its complementarity with RFP-pSB1C3 in a double transformation experiment. Both vectors use a different selection marker (chloramphenicol in pSB1C3 vs. ampicillin in pBluescript) (SnapGene, 2014), a different class of origin of replication (pMB1 derivative in pSB1C3 (Škrlj *et al*, 2009) vs. f1 phage origin in pBluescript), and a experimentally-viable copy number (100-300 copies in pSB1C3 (Škrlj *et al*, 2009) vs. 500-700 copies in pBluescript (Mayer, 1995)), given that the quantity of ribozymes is needed in excess in comparison to the RFP mRNA for efficient inactivation.

In a similar vein, in order to maximize the degradation of RFP transcripts, the expression of ribozymes was ensured with the balancing of relative strengths of the promoters of both ribozyme and RFP cassettes. In fact, the relative promoter strengths of the three promoters used (Part Numbers: BBa_R0040, BBa_R0010, BBa_J23101) were considered in order to allow for a significantly large ratio of ribozyme:RFP mRNA expression (Kelly *et al*, 2009). The transcriptionally-regulated Tet and Lac promoters were also utilized as a part of the design of the XNOR logic gate in order to exploit their tunable levels expression based on the concentration of added anhydrotetracycline and IPTG, which would directly allow for the control and fine-tuning of the ribozyme:RFP mRNA ratio in future experiments. In fact, the reason for the use of the desired DH5αZ1 was due to its genomic expression of the Tet and Lac repressors (Kawe et al, 2009).

After the transformation of the DH5α strain with the ligation products, the cultures were miniprepped and run on an agarose gel, as can be seen in Figure 19. The expected band sizes for lanes 2, 3 and 4 are approximately 2900bp, 3000bp, and 3400bp, representing the three ribozyme expression vectors. Observation of the gel reveals the presence of a single band in each lane at approximately 3000bp, likely indicating the correct insertion of the proper ribozyme cassettes, given no other possible inserts of that size exist. An extra band can be seen at approximately 6000bp in lane 2.

The spectrophotometric assay involving the absorbance measurement at 504nm for RFP normaling for the cell density observed at 600nm was shown to be successful by an

iGEM 2013 team (iGEM HIT-Habin, 2013). Given the success of their experiment and the more timely access to access to a spectrophotometer as opposed to a spectrofluorometer, this approach was taken as an assay for the degradation of the RFP output by ribozyme-based RNA regulation. The spectrophotometer was blank with LB, the culture media used for the experiment. The significant difference in 504nm/600nm absorbance ratio between the strain transformed with pUC19 and that transformed with RFP-pSB1C3 as seen in Figure 21, indicative of the relative strength of the RFP signal, shows that this particular assay is working in that it does detect the presence of RFP in culture. However, the fact that the 504nm/600nm absorbance ratio of the strain transformed with pUC19 with no RFP is approximately 1.3 indicates that there is a significant amount of background noise in the cultures being examined spectrophotometrically, leading to believe that the difference in absorbance ratios may not be directly attributed to the presence of RFP. Furthermore, the 504nm/600nm ratio of the DH5α strain transformed with both the ribozyme and RFP expression vectors was expected to decrease if the lone XNOR ribozyme was in fact succesfully cleaving the RFP mRNA. As is seen in the same figure, there is no marked decrease in ratio associated with this strain, and the ratios of both the RFP and the ribozyme-RFP cultures are both stably fluctuating around the 1.6 ratio.

This leads us to many conclusions about the particular spectrophotometric assay used. Due to the particularly high 504nm/600nm ratio of the pUC19 strain used to assay for background noise, it can be concluded that this assay is not particularly reliable. Meth-

ods to improve the accuracy of this assay would be to us a media with a lesser absorbance and autofluorescence, such as MinA. Another more preferable solution would be the use of a spectrofluorometer as opposed to a spectrophotometer, which would eliminate virtually all background noise experienced in culture, and provide a higher degree of precision. Additionally, it can be concluded that the addition of the XNOR ribozyme in the presence of the RFP transcript did not lower the level of RFP signal output. This can be due to the inaccuracy of the assay itself, the unsuccessful cleavage of the transcript due to the novel ribozyme's design, or many other factors interacting with the binding of the ribozyme to the transcript *in vivo*. It is suggested that the *in vitro* studies are completed in the near future for confirmation of the ribozyme's catalytic activity on the transcript, as well as the testing of the efficacy of the occluder sequences in producing the desired biological XNOR gate.

In summary, the goal of this study was met in that a rational, systematic computational design model was produced for the conception of ribozymes involved in the creation of biological logic gates, and that components of a ribozyme-based XNOR gate were experimentally assayed for *in vivo*. Future work would include the acquirement of the DH5αZ1 strain, the successful transformation of all ribozyme expression vectors into this strain, the improvement of the *in vivo* assay for the XNOR gate, the verification of XNOR gate function in an *in vitro* setting, and perhaps the development of software for the automation of ribozyme design in biological logic gates.

6. Acknowledgements

Dr. Luc Varin (Concordia University) - for his supervision in the lab, his great advice and invaluable feedback.

Drs. Vincent Martin and David Walsh (Concordia University) - for taking the time out of your busy schedules as my committee members.

Dr. Nawwaf Kharma (Concordia University) - for his help in the design of this thesis project, his guidance and his encouragement.

Dr. Jonathan Perrault (INRS) - for his technical feedback and support of this project.

The iGEM Concordia 2013 team - for the constant moral support and the friendships built.

7. References

Ahmed, A., and Sharma, Y.D. (2008). Ribozyme cleavage of Plasmodium falciparum gyrase A gene transcript affects the parasite growth. Parasitol. Res. 103, 751–763.

Amarzguioui, M., and Prydz, H. (1998). Hammerhead ribozyme design and application. CMLS, Cell. Mol. Life Sci. 54, 1175–1202.

Baron, R., Lioubashevski, O., Katz, E., Niazov, T., and Willner, I. (2006). Logic Gates and Elementary Computing by Enzymes†. J. Phys. Chem. A 110, 8548–8553.

Bi, S., Yan, Y., Hao, S., and Zhang, S. (2010). Colorimetric Logic Gates Based on Supramolecular DNAzyme Structures. Angewandte Chemie 122, 4540–4544.

Bronson, J.E., Mazur, W.W., and Cornish, V.W. (2008). Transcription factor logic using chemical complementation. Molecular BioSystems 4, 56.

Busch, A., Richter, A.S., and Backofen, R. (2008). IntaRNA: efficient prediction of bacterial sRNA targets incorporating target site accessibility and seed regions. Bioinformatics 24, 2849–2856.

Carbonell, A., Flores, R., and Gago, S. (2011). Trans-cleaving hammerhead ribozymes with tertiary stabilizing motifs: in vitro and in vivo activity against a structured viroid RNA. Nucl. Acids Res. 39, 2432–2444.

Concordia University Department of Biology (2014). BIOL466 Laboratory Manual.

Deonarine, A.S., Clark, S.M., and Konermann, L. (2003). Implementation of a multifunctional logic gate based on folding/unfolding transitions of a protein. Future Generation Computer Systems 19, 87–97.

Elbaz, J., Lioubashevski, O., Wang, F., Remacle, F., Levine, R.D., and Willner, I. (2010). DNA computing circuits using libraries of DNAzyme subunits. Nat Nano 5, 417–422.

Ferbeyre, G., Bratty, J., Chen, H., and Cedergren, R. (1996). Cell Cycle Arrest Promotes trans-Hammerhead Ribozyme Action in Yeast. J. Biol. Chem. 271, 19318–19323.

Gasiūnaitė, L., Lewicka, A., Pashkuleva, H., Villanueva, H., Thornton, H., Trubitsyna, M., and French, C. (2013). GenBrick – A Rapid Multi-Part Assembly Method for BioBricks.

Hampel, A., and Cowan, J.A. (1997). A unique mechanism for RNA catalysis: the role of metal cofactors in hairpin ribozyme cleavage. Chemistry & Biology 4, 513–517.

iGEM HIT-Harbin. (2013). B-POM: Biological Proportional Operational Mu-Circuit. Accessed in April 2014 at http://2013.igem.org/Team:HIT-Harbin.

Kalweit, A., and Hammann, C. (2013). G17-modified hammerhead ribozymes are active in vitro and in vivo. RNA 19, 1595–1604.

Kawe, M., Horn, U., and Plückthun, A. (2009). Facile promoter deletion in Escherichia coli in response to leaky expression of very robust and benign proteins from common expression vectors. Microbial Cell Factories 8, 8.

Kelly, J.R., Rubin, A.J., Davis, J.H., Ajo-Franklin, C.M., Cumbers, J., Czar, M.J., Mora, K. de, Glieberman, A.L., Monie, D.D., and Endy, D. (2009). Measuring the activity of BioBrick promoters using an in vivo reference standard. Journal of Biological Engineering 3, 4.

Madden, T. (2003). The BLAST Sequence Analysis Tool. The NCBI Handbook. National Center for Biotechnology Information, Chapter 16. Available at http://www.ncbi.nlm.nih.gov/books/NBK21097/

Mayer, M.P. (1995). A new set of useful cloning and expression vectors derived from pBlueScript. Gene 163, 41–46.

Müller-Kuller, T., Capalbo, G., Klebba, C., Engels, J.W., and Klein, S.A. (2009). Identification and characterization of a highly efficient anti-HIV pol hammerhead ribozyme. Oligonucleotides 19, 265–272.

Okamoto, A., Tanaka, K., and Saito, I. (2004). DNA Logic Gates. J. Am. Chem. Soc. 126, 9458–9463.

Olson, K.E., and Müller, U.F. (2012). An in vivo selection method to optimize trans-splicing ribozymes. RNA 18, 581–589.

Owczarzy, R., Tataurov, A.V., Wu, Y., Manthey, J.A., McQuisten, K.A., Almabrazi, H.G., Pedersen, K.F., Lin, Y., Garretson, J., McEntaggart, N.O., et al. (2008). IDT SciTools: a suite for analysis and design of nucleic acid oligomers. Nucleic Acids Res. 36, W163–169.

Qian, L., and Winfree, E. (2011). Scaling Up Digital Circuit Computation with DNA Strand Displacement Cascades. Science 332, 1196–1201.

Richter, A.S., Schleberger, C., Backofen, R., and Steglich, C. (2010). Seed-based IntaRNA prediction combined with GFP-reporter system identifies mRNA targets of the small RNA Yfr1. Bioinformatics 26, 1–5.

Saksmerprome, V., Roychowdhury-Saha, M., Jayasena, S., Khvorova, A., and Burke, D.H. (2004). Artificial tertiary motifs stabilize trans-cleaving hammerhead ribozymes under conditions of submillimolar divalent ions and high temperatures. RNA 10, 1916–1924.

Salehi-Ashtiani, K., and Szostak, J.W. (2001). In vitro evolution suggests multiple origins for the hammerhead ribozyme. Nature 414, 82–84.

Seelig, G., Soloveichik, D., Zhang, D.Y., and Winfree, E. (2006). Enzyme-Free Nucleic Acid Logic Circuits. Science 314, 1585–1588.

Škrlj, N., Erčulj, N., and Dolinar, M. (2009). A versatile bacterial expression vector based on the synthetic biology plasmid pSB1. Protein Expression and Purification 64, 198–204.

Snapgene. (2014). pBluescript II KS(+). Plasmid Files. Resources. Available at http://www.snapgene.com/resources/plasmid_files/image_consortium_plasmids/pBluescript_II_KS(+)/.

Snapgene. (2014). pSB1C3. Plasmid Files. Resources. http://www.snapgene.com/resources/plasmid_files/basic_cloning_vectors/pSB1C3/.

Strack, G., Pita, M., Ornatska, M., and Katz, E. (2008). Boolean Logic Gates that Use Enzymes as Input Signals. ChemBioChem 9, 1260–1266.

Trevors, J. t. (1986). Plasmid curing in bacteria. FEMS Microbiology Letters 32, 149–157.

Vincze, T., Posfai, J., and Roberts, R.J. (2003). NEBcutter: a program to cleave DNA with restriction enzymes. Nucleic Acids Res 31, 3688–3691.

Willner, I., Shlyahovsky, B., Zayats, M., and Willner, B. (2008). DNAzymes for sensing, nanobiotechnology and logic gate applications. Chemical Society Reviews 37, 1153.

Win, M.N., Liang, J.C., and Smolke, C.D. (2009). Frameworks for Programming Biological Function through RNA Parts and Devices. Chemistry & Biology 16, 298–310.

Zhu, J., Li, T., Zhang, L., Dong, S., and Wang, E. (2011). G-quadruplex DNAzyme based molecular catalytic beacon for label-free colorimetric logic gates. Biomaterials 32, 7318–7324.

Zuker, M. (2003). Mfold web server for nucleic acid folding and hybridization prediction. Nucl. Acids Res. 31, 3406–3415.